



HAL
open science

Gelation of whey protein fractal aggregates induced by the interplay between added HCl, CaCl₂ and NaCl

Anna Kharlamova, Taco Nicolai, Christophe Chassenieux

► **To cite this version:**

Anna Kharlamova, Taco Nicolai, Christophe Chassenieux. Gelation of whey protein fractal aggregates induced by the interplay between added HCl, CaCl₂ and NaCl. *International Dairy Journal*, 2020, 111, pp.104824. 10.1016/j.idairyj.2020.104824 . hal-02983931

HAL Id: hal-02983931

<https://hal.inrae.fr/hal-02983931>

Submitted on 30 Oct 2020

HAL is a multi-disciplinary open access archive for the deposit and dissemination of scientific research documents, whether they are published or not. The documents may come from teaching and research institutions in France or abroad, or from public or private research centers.

L'archive ouverte pluridisciplinaire **HAL**, est destinée au dépôt et à la diffusion de documents scientifiques de niveau recherche, publiés ou non, émanant des établissements d'enseignement et de recherche français ou étrangers, des laboratoires publics ou privés.



Distributed under a Creative Commons Attribution - NonCommercial - NoDerivatives 4.0 International License



Gelation of whey protein fractal aggregates induced by the interplay between added HCl, CaCl₂ and NaCl

Anna Kharlamova^{a, b, *}, Taco Nicolai^a, Christophe Chassenieux^a

^a Le Mans Université, IMMM UMR-CNRS 6283, Polymères, Colloïdes et Interfaces, 72085 Le Mans, cedex 9, France

^b INRAE, Institut Agro, STLO, F-35000 Rennes, France

ARTICLE INFO

Article history:

Received 13 April 2020

Received in revised form

22 July 2020

Accepted 23 July 2020

Available online 7 August 2020

ABSTRACT

Gelation of whey protein fractal aggregates was induced by simultaneously adding salt (CaCl₂ or NaCl) and acid (HCl). Further, simultaneous addition of both specifically binding (Ca²⁺) and non-binding (Na⁺) cations was studied at a fixed protein charge density. The effect of adding mixtures of ions on pH, gelation kinetics, elastic modulus and gel microstructure was investigated. For all studied systems the time of gelation (t_g) had an Arrhenius dependence on temperature, characterised by an activation energy (E_a). The value of E_a depended on the type and concentration of added ions. The elastic modulus of gels was found to be independent of the ion composition, reaching 0.2–0.3 kPa at a protein concentration of 40 g L⁻¹ and 1 kPa at 60 g L⁻¹. At conditions of strong electrostatic repulsion between aggregates, addition of NaCl reduced t_g . However, when the repulsions were weak, further addition of NaCl increased t_g .

© 2020 Elsevier Ltd. All rights reserved.

1. Introduction

Milk whey protein is one of the most studied food proteins as it is known for its excellent functional and nutritional properties. Various applications of whey protein have been investigated, such as adjustment of viscosity, gelation, film formation, protein enrichment (Foegeding et al., 2002; Kilara & Vaghela, 2018; Nicolai et al., 2011; Nicolai & Durand, 2013). The proteins found in milk whey are compact globular proteins represented mostly by α -lactalbumin and β -lactoglobulin (de Wit, 1998). The functional properties of globular proteins can be improved by thermal treatment. Upon heating, globular proteins denature and then aggregate due to a higher accessibility of the active sites (Brodkorb et al., 2016; Clark & Lee-Tuffnell, 1998; Nicolai et al., 2011). If the protein concentration (C) is sufficiently high, this process results in gelation. However, if C is below the critical gelation concentration, this process leads to formation of stable suspensions of protein aggregates (Mehalebi et al., 2008; Renard & Lefebvre, 1992). These aggregates can have different morphologies, depending primarily on the magnitude of the net protein charge (α) (Jung et al., 2008).

By varying α , fibrils, microgels and fractal aggregates can be produced from β -lactoglobulin and whey protein isolate (WPI) during heating in aqueous solutions (Jung et al., 2008). Fibrils are long rigid strands produced at pH 2, when the proteins are strongly positively charged (Aymard et al., 1999; Bolder et al., 2006). However, their application in food products seems limited due to the difficulty of manufacturing on an industrial scale (Brodkorb et al., 2016; Cao & Mezzenga, 2019).

Microgels are dense and relatively uniform aggregates formed in two narrow pH regions around the isoionic point (Donato et al., 2009; Nicolai, 2016; Phan-Xuan et al., 2011; Schmitt et al., 2007). For instance, Schmitt et al. (2009) found that microgels formed at pH 6.1–5.8 and 4.3–4.6 for 10 g L⁻¹ solutions of dialysed β -Ig. However, the pH range for microgel formation varies with protein concentration, protein composition and especially presence of divalent cations such as Ca²⁺ (Phan-Xuan et al., 2013, 2014). The latter specifically bind to the proteins (Zittle et al., 1957) and thereby reduce the effective net charge density of the proteins.

Fractal aggregates (or, simply, fractals) are formed when the proteins have both a relatively high net negative charge (pH > 6.2) and a low mineral (especially calcium) content. They can be formed with hydrodynamic radii ranging between $R_h \approx 30$ nm (so-called primary aggregates) to larger than 500 nm (Inthavong et al., 2016), depending mostly on protein concentration and the ionic strength. The primary aggregates are relatively monodisperse in size, but

* Corresponding author. Tel.: +33 2 43 83 31 39.

E-mail address: anna-kharlamova@yandex.ru (A. Kharlamova).

become increasingly polydisperse as the size increases. Fractal aggregates of different sizes have a self-similar structure for which the weight-average molar mass (M_w) increases with increasing radius of gyration (R_g) following a power law: $M_w \propto R_g^{d_f}$, where d_f is the so-called fractal dimension (Sorensen, 2001); $d_f = 1.7$ and 2.0 were found for fractals formed by WPI in salt-free solutions and 0.1 M NaCl, respectively (Mahmoudi et al., 2007; Mehalebi et al., 2008). As a consequence, the density of fractal aggregates decreases with increasing size.

At the same protein concentration, fractal aggregates give stronger gels compared to microgels, because fractals are less dense and therefore occupy a larger volume fraction (Donato et al., 2011; Kharlamova, Nicolai, & Chassenieux, 2018b). Above pH 6, suspensions of negatively charged fractals are stabilised by electrostatic repulsions. Addition of a salt or an acid reduces the repulsion, which can lead to gelation. In the literature this process was named "cold gelation", because it occurs even at ambient temperatures (Barbut, 1995; Bryant & McClements, 1998). However, it has been shown that acid- and salt-induced gelation of fractal aggregates is a thermally activated process. With increasing temperature, the rate of gelation increases, but the mechanical properties and the microstructure of the gels are independent of the temperature. We previously reported $E_a = 220$ kJ mol⁻¹ for Ca²⁺-induced gelation (Kharlamova et al., 2018b) and $E_a = 155$ kJ mol⁻¹ for acid-induced gelation (Kharlamova, Chassenieux, & Nicolai, 2018a) of WPI fractals. With increasing protein concentration, gels were more homogeneous and the elastic shear modulus (G') was found to increase following a power law ($G' \propto C^3$). Increasing the salt or acid concentration or the size of the WPI fractals increased only the rate of gelation, without influencing the gel properties (Kharlamova et al., 2018a,b). Ako et al. (2010) found $E_a = 70$ kJ mol⁻¹ for gelation of β -lg fractals induced by addition of NaCl. Similar results were obtained for gelation of soy protein isolate fractals induced by NaCl (Chen et al., 2017).

So far cold gelation was studied by acidification in the absence of salt or by adding salt at close to neutral pH. However, in many applications both acid and minerals are added. We are not aware of studies of the combined effects of reducing the pH and adding minerals that were reported in the literature. Therefore, the aim of the present investigation was to study gelation of WPI fractals induced by simultaneous addition of acid and salt or a mixture of salts with monovalent and divalent cations. We investigated the gelation kinetics, the mechanical properties and microstructure of gels formed after addition of: (i) HCl and NaCl, (ii) CaCl₂ and NaCl, (iii) HCl and CaCl₂. Results obtained with these systems yield a better understanding of cold gelation as it is influenced by minerals commonly present in food and, more fundamentally, further the understanding of the interaction of proteins in mixtures with different ions.

2. Materials and methods

2.1. Preparation of WPI aggregates

Fractal aggregates were prepared from whey protein isolate powder purchased from a major milk powder manufacturer (Laval, France). It contained 89 wt% protein, 6 wt% moisture, <0.4 wt% fat, <4 wt% lactose and 2.0 wt% ash. The protein fraction consisted of 70% β -lactoglobulin and 20% α -lactalbumin, the remainder comprising other whey proteins and caseins (as determined by size-exclusion chromatography).

The powder was mixed with Milli-Q water at a protein concentration $C = 13$ – 14 wt% and stirred with a magnetic bar overnight. The pH of this stock solution was approximately 6.3. The

solution was then centrifuged for 1.5–2 h at $50,000 \times g$ (Beckman Coulter, Allegra 64R, Villepinte, France) and filtered through $0.2 \mu\text{m}$ syringe filters (Acrodisc®) to remove a small insoluble fraction that could perturb light scattering measurements. The amount of denatured proteins in the WPI powder that was not incorporated into the aggregates was small (<5%) and was not further considered in this study. The protein content of the stock solution after purification was determined by UV absorption at 278–280 nm using the extinction coefficient $\epsilon = 1.05$ L g⁻¹ cm⁻¹ (UV-Visible spectrophotometer, Jasco, USA). This coefficient was determined by measuring the absorbance of WPI solutions with known concentrations. The purified stock solution contained 0.229 g Ca²⁺, 0.111 g Mg²⁺, 0.37 g K⁺ and 0.1 g Na⁺ per 100 g of protein, as determined by flame spectroscopy using Spectrometer Sherwood 410 (Hemeau Laboratories) for Na⁺ and K⁺ and atomic absorption spectrometer iCE 3000 Series (ThermoFischer Scientific) for Ca²⁺ and Mg²⁺ (Parsons et al., 1975).

The net charge density was adjusted by addition of 2 moles of NaOH per mole of protein (considering weight-average $M_w = 1.75 \times 10^4$ g mol⁻¹ for WPI) and the stock solution was diluted to 70 g L⁻¹. This particular protein concentration was chosen because it allowed preparation of reproducible suspensions of fractals with low viscosity (approximately 10^{-2} Pa s at 20 °C), which simplified their mixing with solutions of HCl, CaCl₂ and NaCl. Fractal aggregates with $R_h \approx 30 \pm 3$ nm were prepared by heating the solution in hermetically sealed glass bottles at 80 °C for 5 h, which ensured complete denaturation of the protein. The fractal aggregate solutions were homogeneous and transparent and were kept in the fridge at 4 °C for no longer than 3 weeks. The size of the aggregates was determined with light scattering analysis as described in Phan-Xuan et al. (2011). The net charge density of the aggregated proteins was found to be $\alpha \approx -8.0$, determined by potentiometric titration performed on 10 g L⁻¹ solutions of aggregates at different NaCl concentrations, as described in Kharlamova et al. (2016).

2.2. Preparation of mixtures of aggregates with acid and salts

The fractal aggregate solutions were mixed with different amounts of HCl, NaCl and CaCl₂ solutions in different combinations. Stock solutions of NaCl (0.1, 1, 3 and 4 M) and CaCl₂ (0.1 and 1 M) in Milli-Q water were prepared gravimetrically from powders purchased from Sigma. Standard solutions of HCl (0.1 and 1 M) were purchased from Sigma. The amount of added NaCl was considered in terms of absolute molar concentration (in mM and M), while HCl and CaCl₂ were added considering the number of protons H⁺ or Ca²⁺ per protein, because these ions specifically bind to the proteins.

Solutions of fractal aggregates with the required amounts of HCl, NaCl and/or CaCl₂ were prepared by slowly adding (drop by drop) solutions of the latter while vortex stirring. To slow down aggregation during preparation, all solutions were cooled and mixed on an ice bath.

2.3. Titration experiments

Potentiometric titration was used to measure the change of the pH as a function of the concentration of the added ions. The experiments were conducted at room temperature (approximately 20 °C) using an automatic titrator (TIM 856, Radiometer Analytical) equipped with a combined pH electrode (Radiometer Analytical pH C2401-8 Combination Red-Rod) and a temperature probe. The electrode was calibrated by a three-point calibration with standard buffers (SI Analytics, 60 FIOLAX ampoules, Germany) in the pH range between 4 and 10. 3 M NaCl and 0.1 M CaCl₂ solutions, used as

titrants, were prepared volumetrically at 20 °C from powders purchased from Sigma. 3 M NaCl and 0.1 M CaCl₂ were added at rates of 0.3 mL min⁻¹ and 0.4 mL min⁻¹, respectively; the addition of the titrants (approximately 8 mL) was achieved within 20–30 min. The volume of the added titrant and the pH were recorded automatically and continuously. The addition of the titrant was conducted while stirring. From several repeated measurements at the same conditions we estimate the uncertainty of the electrode measurements within ±0.1 pH unit.

2.4. Rheological measurements

Rheological measurements were used to study the gelation kinetics and mechanical properties of gels by measuring the evolution of the oscillatory shear moduli as a function of time at a fixed temperature. The measurements were conducted using two stress-controlled rheometers (AR2000 and ARG2, TA Instruments) equipped with cone-plate geometries with radius 20 mm and a Peltier system for temperature control. It was verified that both rheometers gave the same result. Samples cooled on ice were promptly (within approximately 1 min) loaded on the rheometer with the temperature of the plate set to 20 °C and covered with mineral oil to avoid evaporation. The temperature was increased from less than 20 °C to the required value within one minute. The moduli were measured at 0.1 Hz within the linear response regime. From several repeated measurements at the same conditions we estimate the uncertainty of the measurement of the oscillatory shear moduli to be less than 10%.

2.5. Confocal laser scanning microscopy (CLSM)

The structure of gels formed by fractal aggregates with different mineral composition and protein net charge was studied with a Zeiss LSM800 microscope (Carl Zeiss Microscopy GmbH, Jena, Germany) equipped with a 63× water immersion objective lens. Samples of aggregates mixed with acid and salts on an ice bath were labelled by addition of 5 ppm of rhodamine B (Merck, Germany), placed on cavity slides, sealed with a cover slip and heated at 80 °C on a rack placed in a water bath. The heating was continued until a steady state was reached, i.e., until no change of the structure with heating time was observed.

3. Results

3.1. Gelation of fractal aggregates induced by HCl and NaCl

Gelation of fractal aggregates induced by simultaneous addition of HCl and NaCl was studied in the NaCl concentration range between 0 and 0.5 M for solutions of fractals at 20, 40 and 60 g L⁻¹. 1, 2, 3, and 4 H⁺ per protein was added in the form of HCl, which resulted in a decrease of the initial negative charge density from $\alpha = -8.0$ to -7.0 , -6.0 , -5.0 , and -4.0 , respectively.

The influence of NaCl on the pH at different fixed charge densities of the fractals was studied by titrating with a 3 M NaCl solution (Fig. 1). Initial addition of small amounts of NaCl (20–40 mM) led to a small steep decrease of the pH that levelled off at higher NaCl concentrations. The initial decrease of the pH was larger at more negative α (higher pH) and became negligible at α approaching the iso-ionic point (pI = 5.0) (see the curve at $\alpha = -2.0$ in Fig. 1). The change of the pH at a fixed α was practically independent of the protein concentration in the studied range (20–60 g L⁻¹).

The decrease of pH with addition of a salt is in accordance with results previously reported in the literature (Kharlamova et al., 2016) and is explained by a small change of the pK_a of the proteins (Salis et al., 2011). However, the effect on the protein net

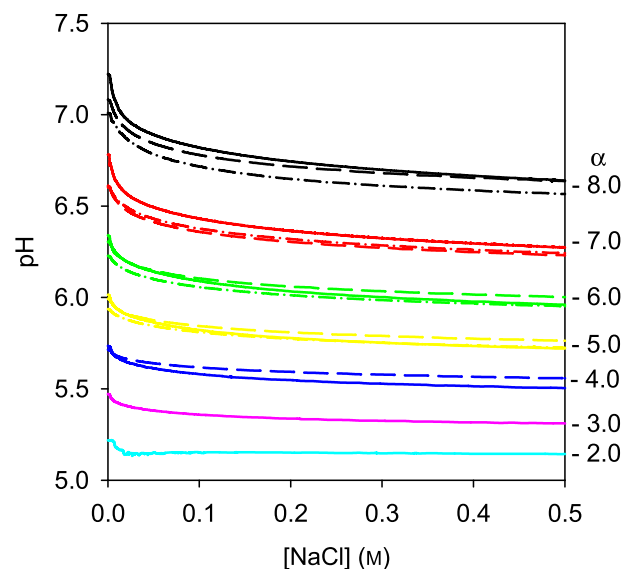


Fig. 1. pH as a function of the NaCl concentration added to suspensions of fractal aggregates at different protein charge densities. Results for three different protein concentrations are shown: —, 20 g L⁻¹; ---, 40 g L⁻¹; - · - ·, 60 g L⁻¹.

charge density, which is the main parameter determining protein aggregation and gelation, is negligible (Kharlamova et al., 2016; Salis et al., 2011).

We determined the minimum NaCl concentration required for gelation at different fixed α and protein concentrations by heating samples in a water bath at 80 °C for 24 h. A series of samples with NaCl concentration increasing with an increment of 10 mM was prepared and heated. Fig. 2 shows the minimal values of NaCl at which gelation occurred.

At the initial charge density $\alpha = -8.0$ (no HCl added) the minimum NaCl concentration required for gelation decreased from 230 mM at 20 g L⁻¹ to 80 and 40 mM at 40 and 60 g L⁻¹,

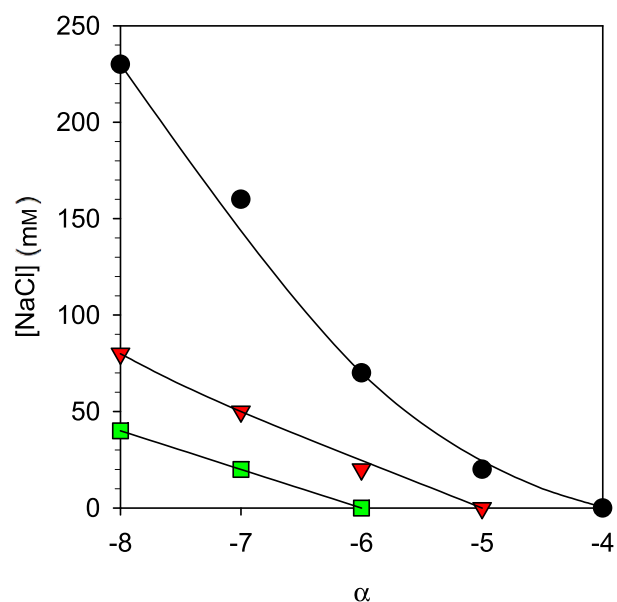


Fig. 2. The minimum NaCl concentration at which gelation occurred after heating for 24 h at 80 °C as a function of α for solutions of fractal aggregates at protein concentrations of: ●, 20 g L⁻¹; ▼, 40 g L⁻¹; ■, 60 g L⁻¹. The lines are guides to the eye.

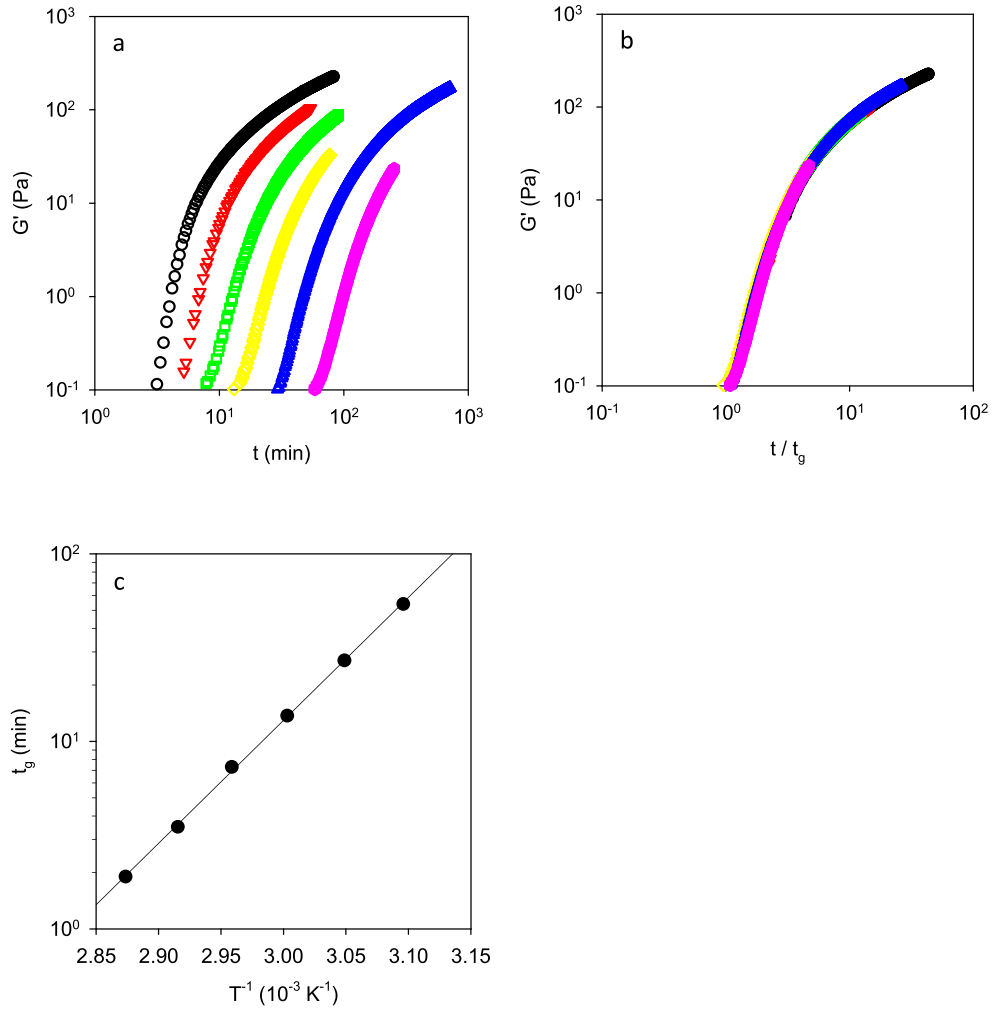


Fig. 3. Evolution (a) of G' at 0.1 Hz with heating time at 50 (○), 55 (△), 60 (◇), 65 (□), 70 (▽) and 75 (○) °C for a solution of fractal aggregates ($R_h = 30$ nm) at $C = 40 \text{ g L}^{-1}$, $\alpha = -5.0$ (3 H^+ per protein) with 0.2 M NaCl ; the same data are presented normalised (b) by the time of gelation t_g ; Arrhenius representation (c) of the temperature dependence of t_g ; the solid line represents the results of a linear least squares fit.

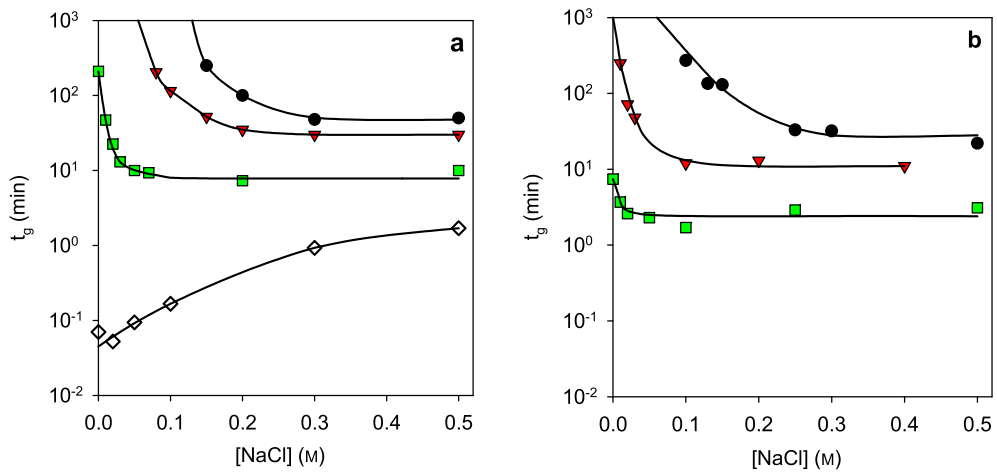


Fig. 4. Gel time determined during heating at 65 °C fractal aggregates at protein concentrations of (a) 40 g L^{-1} and (b) 60 g L^{-1} at different protein charge densities (α) and NaCl concentration. The charge density of -8 (●) was adjusted to -6 (▼), -5 (■) and -4 (◇) by adding 2, 3 and 4 protons per protein, respectively. For $\alpha = -4.0$, t_g was deduced from measurements at lower temperatures using the Arrhenius equation. The lines are guides to the eye.

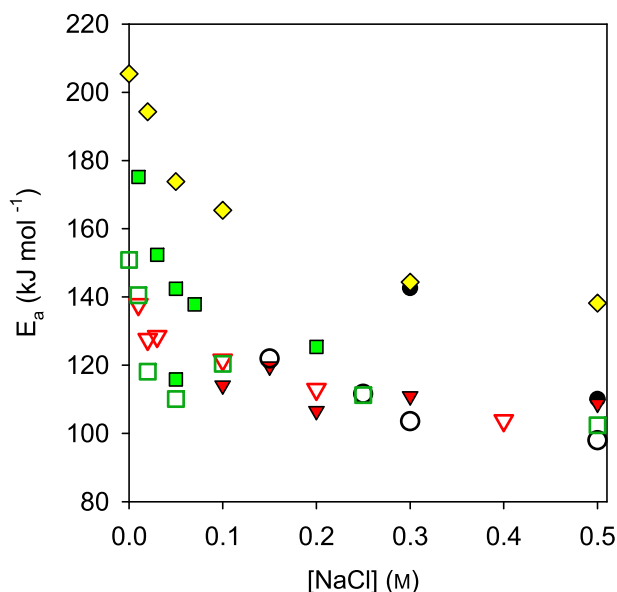


Fig. 5. The activation energy E_a as a function of the NaCl concentration for fractal aggregates at different charge densities (\bullet, \circ –8; $\blacktriangledown, \triangledown$ –6; \blacksquare, \square –5; \blacklozenge, \lozenge –4) and protein concentrations of 40 g L^{-1} (closed symbols) and 60 g L^{-1} (open symbols).

respectively. With addition of 1 H^+ per protein ($\alpha = -7.0$), the minimum NaCl concentration decreased to 160, 50 and 20 mM at 20, 40 and 60 g L^{-1} , respectively. At $\alpha = -6.0$ (2 H^+ added per protein) the solutions at $C = 60 \text{ g L}^{-1}$ gelled even without NaCl, while at least 70 and 20 mM NaCl were required at $C = 20$ and 40 g L^{-1} , respectively. At $\alpha = -5.0$ (3 H^+ per protein) at least 20 mM NaCl was required for gelation at $C = 20 \text{ g L}^{-1}$, but at $C \geq 40 \text{ g L}^{-1}$ the solutions gelled even without NaCl. Finally, at $\alpha = -4.0$ (with addition of 4 H^+ per protein) all samples at $C \geq 20 \text{ g L}^{-1}$ gelled even without NaCl.

Acid-induced gelation of WPI fractals was previously found to be a temperature-activated process with an activation energy (E_a) of 155 kJ mol^{-1} (Kharlamova et al., 2018a). To study the influence of NaCl on the gelation kinetics, samples with different protein concentrations, NaCl concentrations and different α were heated on the rheometer at different fixed temperatures. Fig. 3a shows an example of the evolution of the elastic modulus for a sample containing 40 g L^{-1} of fractals with $\alpha = -5.0$ (3 H^+ added per protein) and 0.2 M NaCl. The elastic modulus increased rapidly at a characteristic time of gelation t_g , defined as the time required to reach the value of $G' = 0.1 \text{ Pa}$. Decrease of the temperature led to slower gelation. However, when the heating time is normalised by t_g , the curves at different temperatures superimpose, implying that the evolution of the elastic modulus is independent of the temperature (see Fig. 3b). By plotting the values of t_g in an Arrhenius plot (Fig. 3c) the value of E_a is obtained from the slope (see Supplementary material for more details).

Similar measurements were conducted on a series of samples at $C = 40 \text{ g L}^{-1}$ and 60 g L^{-1} , at four different charge densities ($\alpha = -8.0, -6.0, -5.0$ and -4.0) in the NaCl concentration range between 0 and 0.5 M . Note that at fixed α the pH decreases with increasing NaCl concentration as was shown in Fig. 1. Fig. 4 shows the values of t_g determined for these systems during heating at 65°C as a function of NaCl concentration. At $\alpha = -8.0$, addition of NaCl up to 0.2 M led to a steep decrease of t_g . At less negative $\alpha = -6.0$ and -5.0 , the same effect is observed up to approximately 0.1 M . With addition of more salt, t_g becomes

practically independent of the NaCl concentration. At a fixed NaCl concentration, t_g decreases with decreasing negative charge (i.e., with decreasing pH) and increasing aggregate concentration. At low salt concentrations, t_g diverges. Although gelation for some systems with very low NaCl concentration was observed during heating at 80°C in glass vials in a water bath, quantification of the values of t_g with the rheometer was difficult as it required a lot of time, especially at temperatures lower than $70\text{--}80^\circ\text{C}$.

At $\alpha = -4.0$ gelation was too fast to determine t_g at 65°C , but it could be deduced at $C = 40 \text{ g L}^{-1}$ from the measurements at lower temperatures using the Arrhenius equation. Interestingly, at this charge density t_g gradually increased by approximately one order of magnitude with addition of up to 0.5 M NaCl.

Gelation was studied at different temperatures. Supplementary material Fig. S1 shows the Arrhenius plots obtained for aggregates at different C , α and NaCl concentrations, from which E_a was calculated for each system. Fig. 5 shows E_a as a function of the NaCl concentration for aggregates at different α at two protein concentrations. At $\alpha = -6.0$ and -5.0 , E_a decreased from approximately 150 kJ mol^{-1} at 0 M NaCl, when gelation was induced purely by acid, to $100\text{--}110 \text{ kJ mol}^{-1}$ in the presence of 0.5 M NaCl. At $\alpha = -8.0$, gelation occurred only after addition of NaCl and $E_a = 110 \pm 10 \text{ kJ mol}^{-1}$.

Remarkably, at $\alpha = -4.0$ (4 H^+ added per protein) the effect of reduction of E_a with addition of NaCl is also observed, but the values of E_a were significantly higher than at more negative charge densities, varying from 205 kJ mol^{-1} at 0 M NaCl to 138 kJ mol^{-1} at 0.5 M NaCl.

The influence of the NaCl concentration on the elastic modulus of the gels at different α was studied by plotting the master curves obtained by time–temperature superposition, i.e., by multiplying the heating time t with a temperature-dependent coefficient a_T with respect to the reference temperature T_{ref} . In Fig. 6a the influence of the NaCl concentration on the elastic modulus of gels at $C = 60 \text{ g L}^{-1}$ at $\alpha = -5.0$ (3 H^+ per protein) is shown at $T_{\text{ref}} = 65^\circ\text{C}$. The same data are normalised by t_g in Fig. 6b, showing that G' of the gels at all NaCl concentrations reached values of the same order of magnitude (1 kPa) after heating for time $t = t_g \times 100$. Master curves for systems at other C and α are shown in Supplementary material Figs. S2 and S3 (for $C = 40 \text{ g L}^{-1}$ and 60 g L^{-1} , respectively). At $C = 40 \text{ g L}^{-1}$, G' rose to approximately 0.01 kPa after heating for $t = t_g \times 10$, and $0.2\text{--}0.3 \text{ kPa}$ after heating for $t = t_g \times 100$ (see Supplementary material Fig. S2).

We noted, however, that the elastic modulus decreased with decreasing NaCl concentration for systems for which a divergence of t_g when the NaCl concentration tended to 0 M was observed in Fig. 4. For instance, for aggregates at $\alpha = -5.0$ and $C = 40 \text{ g L}^{-1}$ at $\text{NaCl} \leq 70 \text{ mM}$ the elastic modulus was lower than at $\text{NaCl} \geq 0.2 \text{ M}$ (Supplementary material Fig. S2f). Similar observations were made for fractals gelling at a more negative $\alpha = -6.0$: G' progressively decreased at $\text{NaCl} \leq 0.1 \text{ M}$ and $\leq 30 \text{ mM}$ NaCl for $C = 40$ and $C = 60 \text{ g L}^{-1}$, respectively (Supplementary material Figs. S2d and S3d). For aggregates at $C = 60 \text{ g L}^{-1}$, $\alpha = -8.0$ and $\geq 0.25 \text{ M}$ NaCl, G' decreased at longer heating due to syneresis (Supplementary material Figs. S3a,b).

The microstructure of the gels was studied at different protein concentrations ($20, 40$ and 60 g L^{-1}), protein charge densities ($\alpha = -8.0, -6.0, -5.0$ and -4.0) and NaCl concentration (between 0 and 0.5 M), see Fig. 7. The aggregate solutions with adjusted C , α and NaCl concentration, prepared on an ice bath, were heated in sealed cavity slides in a water bath at 80°C . Before heating, all samples were homogeneous on the microscopic level (images are

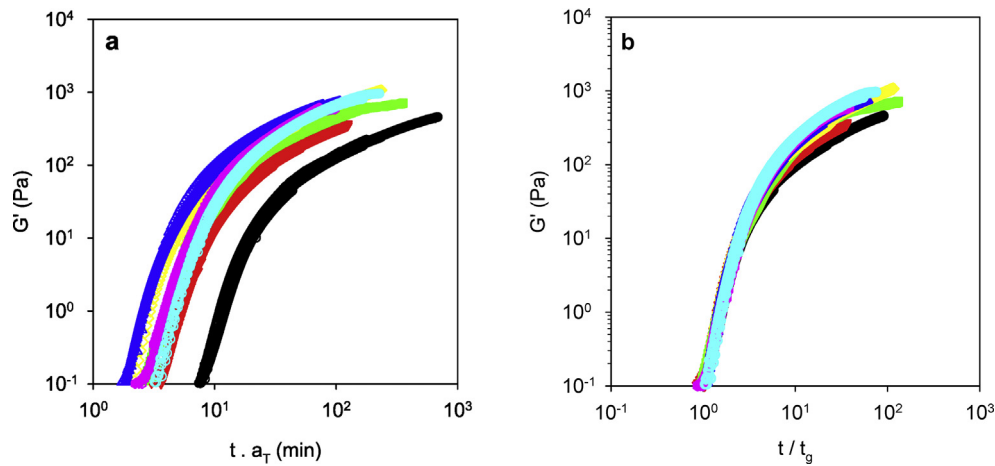


Fig. 6. Master curves (a) of the evolution of G' at 0.1 Hz with heating time for suspensions of fractal aggregates at $C = 60 \text{ g L}^{-1}$ with charge density $\alpha = -5.0$ (3 H^+ per protein) at different NaCl concentrations (\circ , 0 mM; ∇ , 10 mM; \square , 20 mM; \diamond , 50 mM; \triangle , 0.1 M; \circ , 0.25 M; \square , 0.5 M) obtained by time–temperature superposition of curves at different temperatures at $T_{\text{ref.}} = 65 \text{ }^\circ\text{C}$ by multiplying the heating time t by a temperature dependent coefficient a_T ; the same data are presented (b) as a function of t/t_g .

not shown). During heating the microstructure coarsened, but after gelation it no longer changed significantly (results not shown), as we already reported elsewhere for Ca^{2+} - and acid-induced gelation of WPI aggregates (Kharlamova et al., 2018a,b). Fig. 7 shows that the heterogeneity of the gels increased with decreasing C , decreasing negative net protein charge (decreasing pH) and increasing NaCl concentration. With increasing aggregate concentration, gels can be formed with less NaCl and at more negative α , in agreement with results shown in Fig. 2.

3.2. Gelation of fractal aggregates induced by CaCl_2 and NaCl

The study of gelation of fractals induced by simultaneous addition of CaCl_2 and NaCl was done at $C = 40 \text{ g L}^{-1}$. Calcium was added at different molar ratios R between Ca^{2+} and protein. Up to 5 Ca^{2+} ions were added per protein, i.e., up to 11.4 mM, not considering the 1 Ca^{2+} and 0.8 Mg^{2+} ions per protein that were initially present in the powder. Between 0 and 0.5 M NaCl was added.

We first measured the pH of aggregate solutions in the presence of CaCl_2 and NaCl. Fig. 8 shows the change of the pH for solutions of fractals at $C = 40 \text{ g L}^{-1}$ at different fixed R with addition of up to 0.6 M NaCl. Similar to the findings in Fig. 1, addition of up to 0.1 M NaCl resulted in a relatively steep decrease of pH at $R = 0$ –2, followed by a gradual decline. The initial decrease of the pH became smaller with increasing R . At $R = 3$ –5 the steep decrease in the beginning was not observed and pH remained practically the same at all NaCl concentrations.

Samples with 40 g L^{-1} of fractals and different Ca^{2+} and NaCl content were heated on the rheometer at different temperatures in the same manner as shown in Fig. 3a. As for gelation induced by HCl and NaCl, the gelation rate decreased with decreasing temperature and t_g had an Arrhenius temperature dependence (Supplementary material Fig. S4). Fig. 9 shows the values of t_g for gelation at $65 \text{ }^\circ\text{C}$ determined for aggregates with different R and NaCl concentration. At $R = 0$ and 2 an increase of the NaCl concentration initially led to a decrease of t_g , t_g became independent of the NaCl concentration at $\geq 0.2 \text{ M}$ for $R = 0$ and $\geq 0.03 \text{ M}$ for $R = 2$. However, at $R = 3$ –5 addition of NaCl led to an increase of t_g up to approximately 0.1 M and levelled off at higher NaCl concentrations. The same general trends were observed for gelation at other

temperatures in the range between 20 and $80 \text{ }^\circ\text{C}$ (Supplementary material Fig. S5).

From the temperature dependence of t_g we calculated the values of E_a of the gelation process, see Fig. 10. The Arrhenius plots used for the calculation are presented in Supplementary material Fig. S4. With increasing NaCl concentration, E_a gradually decreased from $200 \pm 10 \text{ kJ mol}^{-1}$ when no NaCl was added to $115 \pm 5 \text{ kJ mol}^{-1}$ at 0.5 M NaCl.

Fig. 11 shows the master curves obtained by superposition at $T_{\text{ref.}} = 55 \text{ }^\circ\text{C}$ for aggregates at $C = 40 \text{ g L}^{-1}$ with $R = 4$ at different NaCl concentrations. Fig. 11a shows that gelation slows down with addition of NaCl at this R . When the master curves are normalised by t_g in Fig. 11b, the data approximately superimpose, implying that the NaCl concentration does not influence the elastic modulus of gels at $R = 4$. The elastic modulus reached 0.2–0.3 kPa at $t = t_g \times 100$, close to that of gels prepared at $C = 40 \text{ g L}^{-1}$ with HCl and NaCl (Supplementary material Fig. S2). Similar results were obtained at $R = 3$ and 5 (Supplementary material Fig. S6), but for $R = 2$ some decrease of G' was observed at NaCl $\leq 50 \text{ mM}$ NaCl (Supplementary material Fig. S6b).

The microstructure of the gels at $C = 40 \text{ g L}^{-1}$ with different R and NaCl concentrations is presented in Fig. 12. The heterogeneity increased with increasing R but did not change much with increasing NaCl concentration, except at $R = 0$, where the heterogeneity increased between 0.2 and 0.5 M NaCl.

3.3. Gelation of fractal aggregates induced by HCl and CaCl_2

Gelation of fractals induced by simultaneous addition of HCl and CaCl_2 was studied in a similar manner. Fig. 13a shows the pH of aggregate solutions at $C = 20 \text{ g L}^{-1}$ at different α as a function of R of added Ca^{2+} . The same data are presented as a function of the calcium concentration ($[\text{Ca}^{2+}]$) in Fig. 13b. Titration was conducted at $C = 20 \text{ g L}^{-1}$ so as to avoid gelation during the measurements. Addition of up to 5 Ca^{2+} per protein resulted in a decrease of the pH that was larger at more negative α (less HCl added). At higher R the pH decreased more weakly.

Aggregate solutions at $C = 40 \text{ g L}^{-1}$ at different α and R were heated on the rheometer at fixed temperatures. t_g had an Arrhenius temperature dependence (Supplementary material Fig. S7), similarly to the systems studied above. Fig. 14 shows t_g

20 g L ⁻¹						
	No NaCl	10 mM	50 mM	0.1 M	0.2 M	0.5 M
$\alpha = -8.0$ (0 H ⁺ per prot.)	Do not gel					
$\alpha = -6.0$ (2 H ⁺ per prot.)	Do not gel					
$\alpha = -5.0$ (3 H ⁺ per prot.)	Do not gel					
$\alpha = -4.0$ (4 H ⁺ per prot.)						
40 g L ⁻¹						
	No NaCl	10 mM	50 mM	0.1 M	0.2 M	0.5 M
$\alpha = -8.0$ (0 H ⁺ per prot.)	Do not gel					
$\alpha = -6.0$ (2 H ⁺ per prot.)	Do not gel					
$\alpha = -5.0$ (3 H ⁺ per prot.)						
$\alpha = -4.0$ (4 H ⁺ per prot.)						
60 g L ⁻¹						
	No NaCl	10 mM	50 mM	0.1 M	0.2 M	0.5 M
$\alpha = -8.0$ (0 H ⁺ per prot.)	Do not gel					
$\alpha = -6.0$ (2 H ⁺ per prot.)						
$\alpha = -5.0$ (3 H ⁺ per prot.)						
$\alpha = -4.0$ (4 H ⁺ per prot.)						

Fig. 7. CLSM images (25 $\mu\text{m} \times 25 \mu\text{m}$) obtained for gels formed from fractals at three protein concentrations (20, 40 and 60 g L⁻¹), as a function of α and NaCl concentration, indicated in the figure. Prepared mixtures were sealed in cavity slides and heated at 80 °C until the steady state was reached.

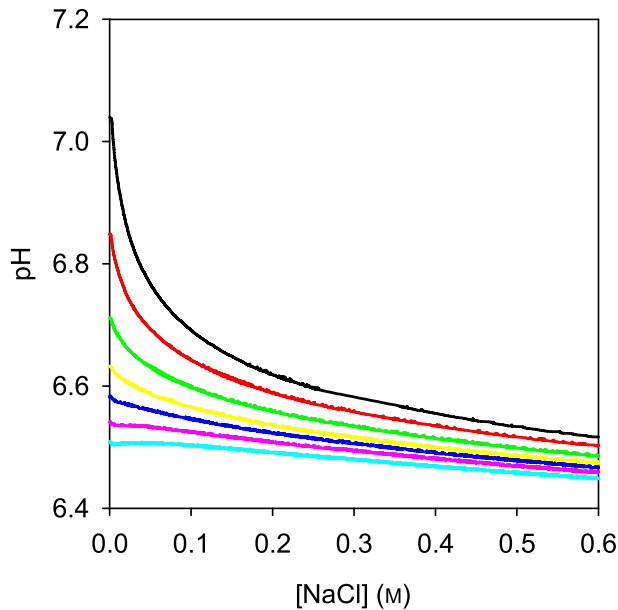


Fig. 8. pH as function of [NaCl] added to solutions of fractals at $C = 40 \text{ g L}^{-1}$ at different R : —, 0; —, 1; —, 2; —, 3; —, 4; —, 5; —, 6. The calcium concentration was fixed before titration by adding $R \text{ Ca}^{2+}$ ions per protein.

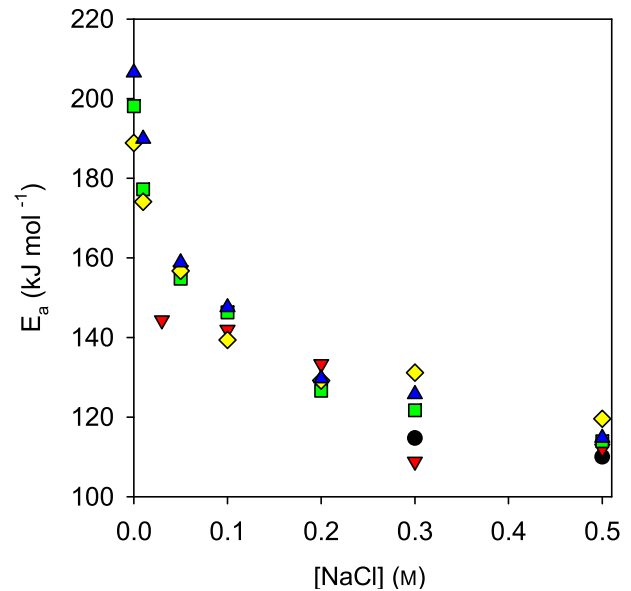


Fig. 10. The activation energy E_a as a function of the NaCl concentration for fractal aggregates at $C = 40 \text{ g L}^{-1}$ and different Ca^{2+} to protein molar ratios R (●, 0; ▼, 2; ■, 3; ◆, 4; ▲, 5).

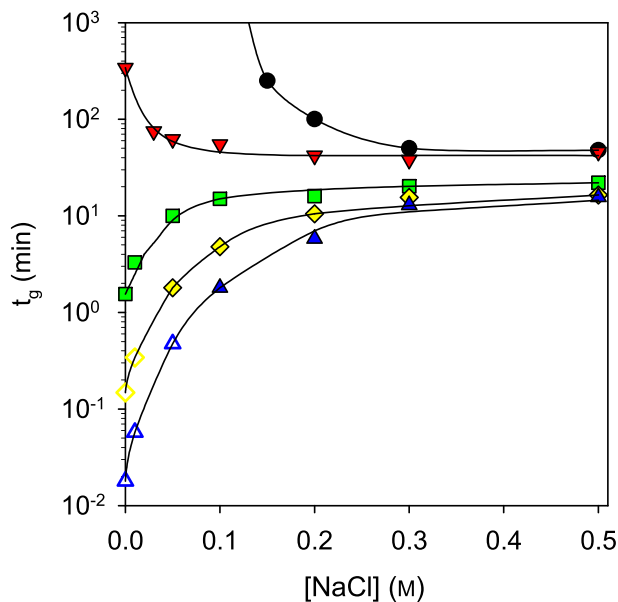


Fig. 9. Gel time (t_g) for gelation at $65 \text{ }^\circ\text{C}$ for fractal aggregates at $C = 40 \text{ g L}^{-1}$ and $\alpha = -8.0$ with different R (●, 0; ▼, 2; ■, 3; ◆, 4; ▲, 5) as a function of the NaCl concentration. Closed symbols correspond to the measured values, whereas the open symbols represent values determined from the measurements at lower temperatures using the Arrhenius equation. The lines are guides to the eye.

at $65 \text{ }^\circ\text{C}$ as a function of R for different α . Some of the values were deduced from the measurements at lower temperatures using the Arrhenius equation (empty symbols). Both addition of Ca^{2+} and H^+ led to a steep decrease of t_g . Decrease of t_g with

increasing R was more important at less negative values of α (i.e., at lower pH).

By varying R between 0 and 5 and α between -8.0 and -4.0 the gelation time could be varied by nine orders of magnitude. The rate of gelation at higher concentrations of Ca^{2+} and H^+ was too fast even at low temperatures. Similar results were obtained for gelation at other temperatures in the range between 20 and $80 \text{ }^\circ\text{C}$ (Supplementary material Fig. S8).

Fig. 15 shows the values of E_a obtained as a function of R at different α . We cannot conclude on any dependency of E_a on R and α . The values of E_a show a significant spread and are mostly found in the range $E_a = 200 \pm 20 \text{ kJ mol}^{-1}$.

Similarly to the systems described in sections 3.1 and 3.2, the elastic modulus was found to be independent of α and R over the range examined. At 40 g L^{-1} G' reached $0.2\text{--}0.3 \text{ kPa}$ after $t = t_g \times 100$ (Supplementary material Fig. S9).

Fig. 16 shows the microstructure of the gels at $C = 40 \text{ g L}^{-1}$ as a function of α and R . The heterogeneity increased with increasing R and decreasing negative charge. At $\alpha = -4.0$ addition of calcium at $R \geq 3$ resulted in immediate gelation in spite of the low temperature at which samples were prepared, which produced macroscopically heterogeneous gels.

4. Discussion

Fractal aggregates are formed at conditions at which the proteins have a high negative charge, rendering suspensions of fractals stable during storage. The negative charge can be reduced by addition of acid or salt, which can lead to gelation (Fig. 17). Most protons from added acid bind to the proteins, which results in a decrease of the negative net charge of proteins. In the case of salt, the mechanism of reduction of electrostatic repulsions depends on whether the ions bind specifically to the proteins or only screen the interaction. Addition of divalent cations like Ca^{2+} that bind

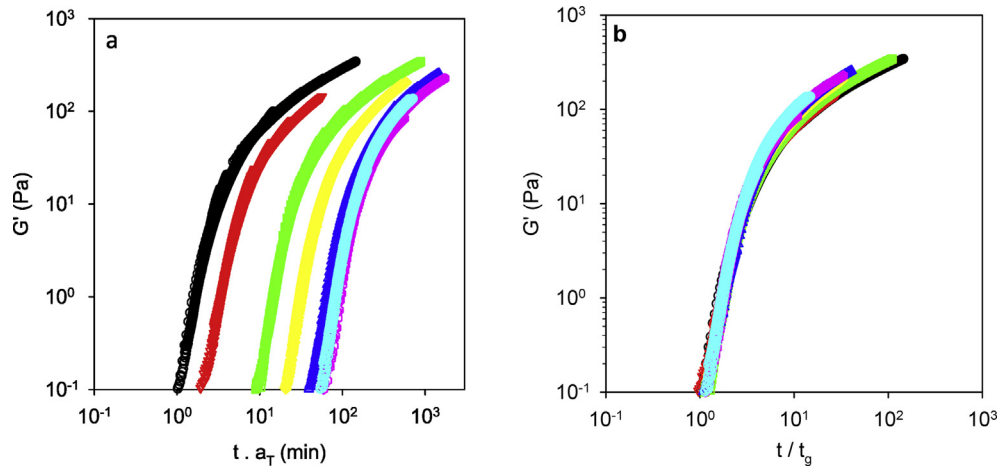


Fig. 11. Master curves (a) of the evolution of G' at 0.1 Hz with heating time for suspensions of fractal aggregates at $C = 40 \text{ g L}^{-1}$ with $R = 4$ at different NaCl concentrations (\circ , 0 mM; ∇ , 10 mM; \square , 50 mM; \diamond , 0.1 M; \triangle , 0.2 M; \circ , 0.3 M; \circ , 0.5 M) obtained by time–temperature superposition at $T_{\text{ref.}} = 55 \text{ }^\circ\text{C}$; the same data are presented (b) as a function of t/t_g .

	No NaCl	10 mM	50 mM	0.1 M	0.2 M	0.5 M
0 Ca^{2+}	Do not gel					
1 Ca^{2+}	Do not gel					
2 Ca^{2+}						
3 Ca^{2+}						
4 Ca^{2+}						

Fig. 12. CLSM images ($25 \mu\text{m} \times 25 \mu\text{m}$) obtained for gels at $C = 40 \text{ g L}^{-1}$ at $\alpha = -8.0$, at different calcium to protein ratios R and NaCl concentrations, indicated in the figure. The mixtures prepared on an ice bath and sealed in cavity slides were heated at $80 \text{ }^\circ\text{C}$ until the steady state was reached.

specifically to proteins leads to a reduction of the effective protein charge density. We previously reported for fractal aggregates produced in the same way from the same WPI powder that up to 3 Ca^{2+} ions can bind per protein in fractal aggregates (Kharlamova et al., 2018b). Excess of added calcium contributes to the screening of electrostatic interactions. In the case of salts not containing specifically binding ions, like NaCl, gelation happens due to the screening of electrostatic interactions only.

The relatively small decrease of the pH with addition of NaCl to protein solutions at different α (Fig. 1) has been reported in the literature (Kharlamova et al., 2016) and is explained by a minor change of the dissociation constant due to the electrostatic screening. The effect is progressively less important when α approaches zero and is not observed at the isoionic point (IIP \approx pH 5.0), where the net protein charge is zero. The effect of NaCl is seen in Fig. 8 for aggregates with $R \leq 2$ and is negligible at $R > 2$ when the effective charge density is much reduced due to specific binding of calcium ions. The weak decrease of pH with addition of small amounts of Ca^{2+} seen in Fig. 13 is explained by binding of calcium ions to the protein.

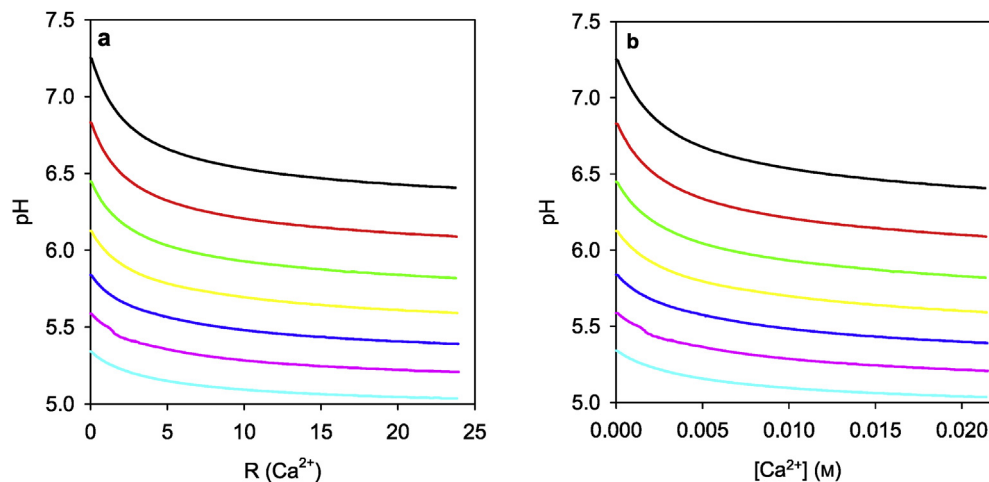


Fig. 13. pH as function (a) of the molar ratio between added Ca^{2+} and protein for suspensions of fractals at $C = 20 \text{ g L}^{-1}$ and different α (—, -8.0 ; —, -7.0 ; —, -6.0 ; —, -5.0 ; —, -4.0 ; —, -3.0 ; —, -2.0). The same data are shown (b) as function of the absolute concentration of added Ca^{2+} .

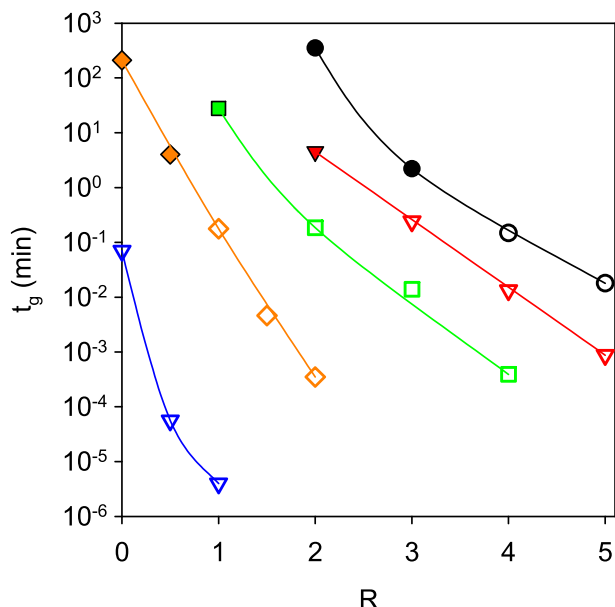


Fig. 14. Gel time determined during heating at 65 °C for fractal aggregates at 40 g L⁻¹ and different α (●, ○, -8.0; ▼, ▽, -7.0; ■, □, -6.0; ◆, ◇, -5.0; ▲, △, -4.0) as function of R. Closed symbols correspond to the measured values and open symbols correspond to values determined from measurements at lower temperatures using the Arrhenius equation.

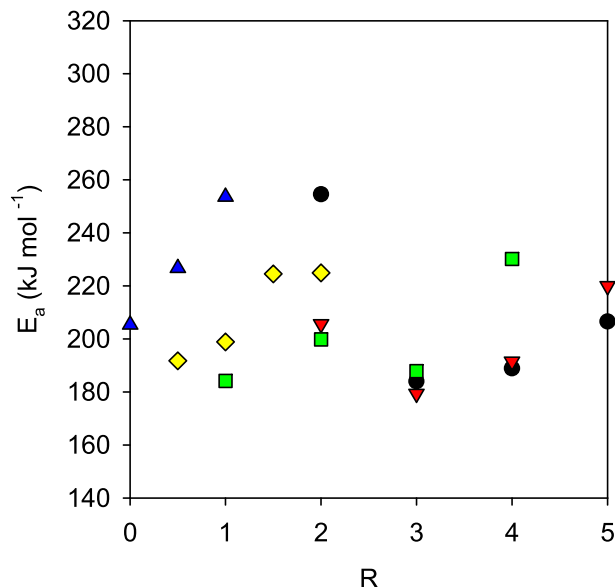


Fig. 15. E_a as function of R for fractal aggregates at $C = 40 \text{ g L}^{-1}$ at different charge densities: (●, ○, -8.0; ▼, ▽, -7.0; ■, □, -6.0; ◆, ◇, -5.0; ▲, △, -4.0).

For gelation of fractals induced by simultaneous addition of HCl and NaCl or CaCl₂ and NaCl, we have observed in both cases a decrease of E_a from approximately 150 and 200 kJ mol⁻¹, respectively, to $110 \pm 10 \text{ kJ mol}^{-1}$ with increasing NaCl concentration from 0 to 0.5 M. We previously reported the values of 155 kJ mol⁻¹ (Kharlamova et al., 2018a) and 210 kJ mol⁻¹ (Kharlamova et al., 2018b) for acid- and Ca²⁺-induced gelation, respectively.

Therefore, we may conclude that with increasing NaCl concentration, gelation gradually shifts from being caused by a reduction of the effective charge density to being caused by screening. Here we found $E_a = 110 \pm 10 \text{ kJ mol}^{-1}$ for gelation of WPI fractals induced by only NaCl. $E_a = 70 \text{ kJ mol}^{-1}$ and 72 kJ mol^{-1} were previously reported for NaCl-induced gelation of β -lg fractal aggregates (Ako et al., 2010) and soy protein isolate fractal aggregates (Chen et al., 2017), respectively.

For gelation induced by addition of both HCl and NaCl we found that E_a did not depend on α in the range between -8.0 and -5.0, but had systematically higher values at $\alpha = -4.0$. We do not have an explanation for this observation. In particular, it is difficult to understand why E_a increased when the net charge density, and therefore the electrostatic repulsion, was smaller.

Interestingly, it was found that addition of NaCl decreased t_g only at high negative α and at small R. At $\alpha = -4.0$ and at $R \geq 3$ addition of NaCl was found to cause an increase of t_g (see Figs. 4 and 9). Addition of NaCl favours gelation by screening electrostatic repulsions. However, it appears that when the effective charge density is sufficiently reduced by binding of H⁺ or Ca²⁺, addition of NaCl slows down gelation. One possible explanation is that addition of NaCl screens opposite charge interactions, which could play a role in gelation when the effective net protein charge is small. We note that even when no CaCl₂ was added, 1 Ca²⁺ and 0.8 Mg²⁺ were present per protein.

As might be expected, the rate of gelation induced by simultaneous addition of HCl and CaCl₂ increased dramatically with increasing amount of both components in the whole studied range, because both lead to a reduction of the effective protein charge density.

This study showed that, in general, the value of the elastic modulus of the gels increases with increasing protein concentration, and is independent of the charge density and the salt content. A similar finding had already been reported for pure acid- and calcium-induced gelation (Kharlamova et al., 2018a,b). However, we noted a tendency to a reduction of the elastic modulus with increasing NaCl concentration when the proteins were strongly negatively charged (at $\alpha = -8.0$), which we explained by syneresis. The elastic modulus was also found to decrease when very small amounts of HCl/CaCl₂/NaCl were added, implying that full gelation requires reduction of electrostatic repulsions to below some critical value.

As might be expected, the microstructure of the gels was more heterogeneous when the electrostatic repulsion was weaker. However, no clear relationship between the microstructure as observed by CLSM and the elastic modulus of the gels was found. Clearly, the gel stiffness cannot be understood solely by considering the microstructure and one needs to also consider the bonds at the molecular length scale. Even if the microstructure is the same, the force required to deform the strands or crosslinks of the network may not be the same, because that will also depend on the type of bonds.

Here we did not study the influence of the aggregate size to limit the number of studied parameters. Previously we found the elastic moduli, the structure and E_a to be independent of the aggregate size, at least in the range of R_h between 30 and 200 nm (Kharlamova et al., 2018a,b). However, an approximately 10-fold increase of the gelation rate was found with increasing R_h from 30 to 200 nm for aggregates at $C = 60 \text{ g L}^{-1}$ at $\alpha = -4.0$ (Kharlamova et al., 2018a). We suggested that during gelation smaller aggregates first aggregate into larger ones before forming a network, which explains the difference in the gelation rate.

	R					
	0	1	2	3	4	5
$\alpha = -8.0$ (0 H ⁺ added)	Do not gel					
$\alpha = -7.0$ (1 H ⁺ added)	Does not gel					
$\alpha = -6.0$ (2 H ⁺ added)	Does not gel					
$\alpha = -5.0$ (3 H ⁺ added)						
$\alpha = -4.0$ (4 H ⁺ added)				Immediate gelation even at low temperatures		

Fig. 16. CLSM images (25 $\mu\text{m} \times 25 \mu\text{m}$) obtained for suspensions of fractals at $C = 40 \text{ g L}^{-1}$ at different α and R as indicated in the figure. The mixtures were prepared on ice, sealed in cavity slides, and subsequently heated in a water bath at 80 °C until steady state was reached.

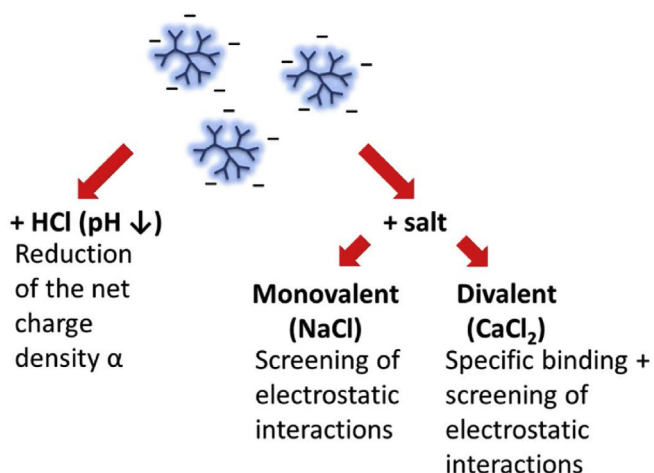


Fig. 17. Reduction of electrostatic interactions between fractal protein aggregates.

5. Conclusions

Gelation of fractal aggregates can be induced by addition of ions that either bind specifically to proteins (H⁺, Ca²⁺) reducing the effective net charge density of proteins or do not bind specifically to proteins (Na⁺), but screen the electrostatic repulsions. In all cases gelation was found to have an Arrhenius temperature dependence, characterised by E_a . Here $E_a = 110 \pm 10 \text{ kJ mol}^{-1}$ was found for gelation of fractals induced by addition of NaCl to be compared with $E_a = 210 \text{ kJ mol}^{-1}$ and 155 kJ mol^{-1} for Ca²⁺- and H⁺-induced gelation that we reported elsewhere. From the dependence of E_a on the NaCl concentration we deduced that when gelation is induced by mixtures of HCl and NaCl or CaCl₂ and NaCl, there is with increasing NaCl concentration a shift from gelation controlled by specifically binding ions (H⁺ and Ca²⁺) to gelation controlled by

NaCl. For gelation induced by a mixture of HCl and CaCl₂, we found that E_a is approximately $200 \pm 20 \text{ kJ mol}^{-1}$ independent of the mineral composition, implying that gelation is mostly controlled by Ca²⁺. The elastic modulus was found to be independent of the mineral content, reaching 0.2–0.3 kPa at $C = 40 \text{ g L}^{-1}$ and approximately 1 kPa at $C = 60 \text{ g L}^{-1}$. Addition of NaCl was found to decrease t_g at conditions where the negative net protein charge was not significantly reduced by specifically binding ions. Otherwise, t_g increased with addition of NaCl. Adding a mixture of specifically binding ions (H⁺ and Ca²⁺) was found to decrease t_g at all studied R and α .

Acknowledgements

Bba association, Le Mans University and the Regional councils of Brittany and Pays de la Loire who funded this work through the interregional PROFIL project, carried out by the association "Pole Agronomique Ouest", are thanked. We also thank Dr. J. Léonil of the INRA for the scientific coordination.

Appendix A. Supplementary data

Supplementary data to this article can be found online at <https://doi.org/10.1016/j.idairyj.2020.104824>.

References

- Ako, K., Nicolai, T., & Durand, D. (2010). Salt-induced gelation of globular protein aggregates: Structure and kinetics. *Biomacromolecules*, 11, 864–871.
- Aymard, P., Nicolai, T., Durand, D., & Clark, A. (1999). Static and dynamic scattering of β -lactoglobulin aggregates formed after heat-induced denaturation at pH 2. *Macromolecules*, 32, 2542–2552.
- Barbut, S. (1995). Effects of calcium level on the structure of pre-heated whey protein isolate gels. *LWT-Food Science and Technology*, 28, 598–603.
- Bolder, S. G., Hendrickx, H., Sagis, L. M. C., & van der Linden, E. (2006). Fibril assemblies in aqueous whey protein mixtures. *Journal of Agricultural and Food Chemistry*, 54, 4229–4234.

- Brodtkorb, A., Croguennec, T., Bouhallab, S., & Kehoe, J. J. (2016). Heat-induced denaturation, aggregation and gelation of whey proteins. In P. L. H. McSweeney, & J. A. O'Mahony (Eds.), *Advanced dairy chemistry* (pp. 155–178). New York, NY, USA: Springer New York.
- Bryant, C. M., & McClements, D. J. (1998). Molecular basis of protein functionality with special consideration of cold-set gels derived from heat-denatured whey. *Trends in Food Science & Technology*, 9, 143–151.
- Cao, Y., & Mezzenga, R. (2019). Food protein amyloid fibrils: Origin, structure, formation, characterization, applications and health implications. *Advances in Colloid and Interface Science*, 269, 334–356.
- Chen, N., Chassenieux, C., & Nicolai, T. (2017). Kinetics of NaCl induced gelation of soy protein aggregates: Effects of temperature, aggregate size, and protein concentration. *Food Hydrocolloids*, 77, 66–74.
- Clark, A. H., & Lee-Tuffnell, C. D. (1998). Gelation of globular proteins. *Functional Properties of Food Macromolecules*, 2, 77–142.
- Donato, L., Kolodziejczyk, E., & Rouvet, M. (2011). Mixtures of whey protein microgels and soluble aggregates as building blocks to control rheology and structure of acid induced cold-set gels. *Food Hydrocolloids*, 25, 734–742.
- Donato, L., Schmitt, C., Bovetto, L., & Rouvet, M. (2009). Mechanism of formation of stable heat-induced β -lactoglobulin microgels. *International Dairy Journal*, 19, 295–306.
- Foegeding, E. A., Davis, J. P., Doucet, D., & McGuffey, M. K. (2002). Advances in modifying and understanding whey protein functionality. *Trends in Food Science & Technology*, 13, 151–159.
- Inthavong, W., Kharlamova, A., Chassenieux, C., & Nicolai, T. (2016). Structure and flow of dense suspensions of protein fractal aggregates in comparison with microgels. *Soft Matter*, 12, 2785–2793.
- Jung, J.-M., Savin, G., Pouzot, M., Schmitt, C., & Mezzenga, R. A. (2008). Structure of heat-induced β -lactoglobulin aggregates and their complexes with sodium-dodecyl sulfate. *Biomacromolecules*, 9, 2477–2486.
- Kharlamova, A., Chassenieux, C., & Nicolai, T. (2018a). Acid-induced gelation of whey protein aggregates: Kinetics, gel structure and rheological properties. *Food Hydrocolloids*, 81, 263–272.
- Kharlamova, A., Inthavong, W., Nicolai, T., & Chassenieux, C. (2016). The effect of aggregation into fractals or microgels on the charge density and the isoionic point of globular proteins. *Food Hydrocolloids*, 60, 470–475.
- Kharlamova, A., Nicolai, T., & Chassenieux, C. (2018b). Calcium-induced gelation of whey protein aggregates: Kinetics, structure and rheological properties. *Food Hydrocolloids*, 79, 145–157.
- Kilara, A., & Vaghela, M. N. (2018). Whey proteins. In R. Y. Yada (Ed.), *Proteins in food processing* (2nd ed., pp. 93–126). Cambridge, UK: Woodhead Publishing.
- Mahmoudi, N., Mehalebi, S., Nicolai, T., Durand, D., & Riaublanc, A. (2007). Light-scattering study of the structure of aggregates and gels formed by heat-denatured whey protein isolate and β -lactoglobulin at neutral pH. *Journal of Agricultural and Food Chemistry*, 55, 3104–3111.
- Mehalebi, S., Nicolai, T., & Durand, D. (2008). Light scattering study of heat-denatured globular protein aggregates. *International Journal of Biological Macromolecules*, 43, 129–135.
- Nicolai, T. (2016). Formation and functionality of self-assembled whey protein microgels. *Colloids and Surfaces B: Biointerfaces*, 137, 32–38.
- Nicolai, T., Britten, M., & Schmitt, C. (2011). β -Lactoglobulin and WPI aggregates: Formation, structure and applications. *Food Hydrocolloids*, 25, 1945–1962.
- Nicolai, T., & Durand, D. (2013). Controlled food protein aggregation for new functionality. *Current Opinion in Colloid & Interface Science*, 18, 249–256.
- Parsons, M. L., Smith, B. W., & Bentley, G. E. (1975). *Handbook of flame spectroscopy*. Boston, MA, USA: Springer US.
- Phan-Xuan, T., Durand, D., Nicolai, T., Donato, L., Schmitt, C., & Bovetto, L. (2011). On the crucial importance of the pH for the formation and self-stabilization of protein microgels and strands. *Langmuir*, 27, 15092–15101.
- Phan-Xuan, T., Durand, D., Nicolai, T., Donato, L., Schmitt, C., & Bovetto, L. (2013). Tuning the structure of protein particles and gels with calcium or sodium ions. *Biomacromolecules*, 14, 1980–1989.
- Phan-Xuan, T., Durand, D., Nicolai, T., Donato, L., Schmitt, C., & Bovetto, L. (2014). Heat induced formation of beta-lactoglobulin microgels driven by addition of calcium ions. *Food Hydrocolloids*, 34, 227–235.
- Renard, D., & Lefebvre, J. (1992). Gelation of globular proteins: Effect of pH and ionic strength on the critical concentration for gel formation. A simple model and its application to β -lactoglobulin Heat-Induced gelation. *International Journal of Biological Macromolecules*, 14, 287–291.
- Salis, A., Boström, M., Medda, L., Cugia, F., Barse, B., Parsons, D. F., Ninham, B. W., & Monduzzi, M. (2011). Measurements and theoretical interpretation of points of zero charge/potential of BSA protein. *Langmuir*, 27, 11597–11604.
- Schmitt, C., Bovay, C., Rouvet, M., Shojaei-Rami, S., & Kolodziejczyk, E. (2007). Whey protein soluble aggregates from heating with NaCl: Physicochemical, interfacial, and foaming properties. *Langmuir*, 23, 4155–4166.
- Schmitt, C., Bovay, C., Vuillomenet, A.-M., Rouvet, M., Bovetto, L., Barbar, R., & Sanchez, C. (2009). Multiscale characterization of individualized β -lactoglobulin microgels formed upon heat treatment under narrow pH range conditions. *Langmuir*, 25, 7899–7909.
- Sorensen, C. M. (2001). Light scattering by fractal aggregates: A review. *Aerosol Science and Technology*, 35, 648–687.
- de Wit, J. N. (1998). Nutritional and functional characteristics of whey proteins in food products. *Journal of Dairy Science*, 81, 597–608.
- Zittle, C. A., DellaMonica, E. S., Rudd, R. K., & Custer, J. H. (1957). The binding of calcium ions by β -lactoglobulin both before and after aggregation by heating in the presence of calcium ions. *Journal of the American Chemical Society*, 79, 4661–4666.